Dynamic electron transfer and intermediate detection in Azurin

Authors*

Huygens-Kamerlingh Onnes Laboratory, Leiden University, RA, Leiden, The Netherlands

E-mail: corresponding_author@physics.leidenuniv.nl

Introduction

Introduction here.

Experimental Section

Protein synthesis

Azurin (wild type) from *Pseudomonas aeruginosa* was expressed in E. Coli and purified as described before[1]. BL21 E.coli was transformed with PGK22 plasmid that has gene for azurin expression. The cells were cultured in luria broth (LB) medium. Then the cells were harvested and resuspended in a 20 % (w/v) sucrose solution in Tris pH 8 buffer containing 1 mM EDTA. The solution was centrifuged at 8000 rpm and the supernatant was collected. Copper sulfate was added to the solution for insertion into the active site of azurin. The unwanted proteins were precipitated by addition of acetic acid until pH 4. Again the turbid solution was centrifuged to separate azurin that remained in the supernatant. The azurin solution was loaded on a CM Sepharose fast flow column and elution was performed in an Akta purifier (GE Healthcare) with a pH gradient from 4 to 6.9 in 50 mM ammonium

acetate. Fractions containing azurin collected and reduced with sodium dithionite. At this moment the solution had both zinc and copper azurin. The azurins were purified in a DEAE sepharose column by a salt gradient of 0 to 50 mMNaCl in Tris pH8 buffer. Fractions containing copper azurin and zinc azurin were collected and concentrated separately. The purity of the samples were checked by sodium dodecyl sulphate (SDS)-polyacrylamide gel electrophoresis (PAGE) and UV/Vis spectroscopy (Cary 50 spectrophotometer, Varian Inc., Agilent Technologies, USA). The azurins appeared on SDS gel page at ∼14 kDa. Both zinc and copper azurin showed a characteristic peak at ∼290 nm while Cu azurin showed an additional broad absorption peak at 620 nm as can be seen in Figure-S2 when oxidized. The ratio $O.D_{628\,\mathrm{nm}}/O.D_{280\,\mathrm{nm}}$ for Cu azurin was 0.56 which indicated that all the azurin molecules had a Cu atom. The concentrated protein was stored at 80 ^{o}C until further use.

Fluorescent labeling

The labeling protocol was based on previous work.[2] ATTO 655 NHS-ester was bought from ATTO-TEC GmbH. The buffer containing azurin was replaced with HEPES pH 8.3 and all the amine containing impurities were removed. ATTO655 was chosen to label the protein because of its stability and light insensitivity in the interested potential range. A mixture of 200 μM azurin and ATTO 655 NHS-ester (ration 1:1) was incubated for 45 min. The NHS-ester group reacts to one of the amine group on the protein. The unreacted dyes were removed with a HiTrap desalting column. The labeled protein was concentrated in Tris pH 8.5 buffer by centrifuging in a 3 kDa Amicon ultra filter. The labeled protein was further purified by an ion exchange chromatography in a 1 mL MonoQ column (GE Health). The different peaks obtained (see Figure S1) correspond to the different number and position of the dye on azurin. The peak-III corresponds to the protein labeled at Lysine122 position.[2] For this position of the dye, the protein construct shows a high fluorescence switching (90%) ratio between oxidized and reduced condition as can be seen in Figure S1. This fraction was chosen for our single-molecule experiment as the two states can be observed easily. The same

protocol was used for Zn azurin labeling and similar peak separation were observed. The fluorescent labeled protein was then reacted with biotin-peg-NHS (MW 3400) in phosphate-buffered saline (PBS) pH 7.4 buffer with a ratio 1:5 to make sure each protein has at least one biotin. The free biotin was then removed by centrifuging in a 3kDa Amicon ultra filter. The biotin on the protein will be used for immobilization on the glass surface.

Functionalization of cover slips

The functionalization of glass surface was followed from a previous work with a little modification.[3] Glass coverslips (Menzel-Glaser, 22 $mm \times 40$ mm, no. 1 thickness) were used for immobilization. The cover slips were sonicated in water (15 min) and acetone (15 min). Then they were rinsed in Milli-Q water several times and incubated in a H2O/NH4OH/H2O2(5:1:1) bath at 70 ^{o}C for burning all the organic impurity on the surface. The coverslips were rinsed several times with water and ethanol and finally stored in ethanol. Before functionalization, the slides were flamed and treated for 30 min with a 1% solution of [3-(2-aminoethyl)aminopropyl]trimethoxysilane in methanol containing 5% glacial acetic acid. This results in the binding of the active hydroxyl groups. The silane is not yet covalently bound. This is obtained by baking the cover slips in an oven at 65 ^{o}C for 3 hours. After this treatment, the cover slips were sonicated for 10 minutes and washed with methanol. Dried with clean nitrogen, they were left in a desiccator overnight. The next day they were treated with a mixture of 5 mg/mL methoxy-peg-N-hydroxysuccinimide (MW 2000, Laysan Bio) and 0.05 mg/mL biotin-peg-N-hydroxysuccinimide (MW 3400, Laysan Bio) in 50 mM phosphate buffered saline (PBS) with pH 7.4. This creates a surface containing biotin and methoxy end groups. The PEG surface prevents nonspecific adsorption of the protein. The slides were dried with gentle flow of nitrogen and stored in a desiccator until further use.

Protein immobilization

The biotin functionalized glass slide was incubated with 20 mM PBS pH 7.4 buffer for 5 min. 100 nM of NeutrAvidin (Thermo Scientific) was incubated for another 15 min and then washed to remove unbound Neutravidin. Then 100 pM of the labeled protein was then incubated for 1 min to get isolated proteins (20 per 100 μm area) on the functionalized glass surface. The unbound proteins were then removed by replacing with a fresh PBS buffer.

Electrochemical-potential control

Once the unbound proteins are removed, a new mixture containing 0.1 mM sodium ascorbate ($[C_6H_7O_6]^-Na^+$) and 0.2 mM potassium ferricyanide ($[Fe(CN)_6]^{3-}$) in 4 mL PBS pH 7.4 was added in the sample holder which contained our initial oxidant and reductant. The electrochemical potential of the solution is obtained from the ratio of oxidant and reductant. The solution potential was controlled with the same electrochemical set up as previously described[4] with little modification. A potentiostat (Model 800B Series Electrochemical Detector, CH Instruments) was used to apply electric potential. A platinum rectangular grid (the total length/ width of the grid is around 2.5 cm) was used as working electrode and pressed onto the sample slide with the help of a small glass slide. Not only is the pressure evenly applied on the grid, but also small confined volumes are formed where the sample slide and glass slide form the 'floor' and 'roof' and the platinum grid forms the 'walls'. A part of the platinum grid was exposed to the solution. These confined volumes are in the order of nanoliters, which makes switching of the elctrochemical potential of the solution possible in a matter of minutes.

Confocal Microscope

Single-molecule measurements were carried out in a home built confocal microscope. The setup was equipped with 635 nm pulsed diode laser (Power Technology, Little Rock, AR,

USA) controlled by a PDL 828 "Sepia II" (PicoQuant) at 40 MHz repetition rate. the laser beam was passed through a narrow-band cleanup filter (Semrock LD01-640/8-25) and coupled to a single-mode optical fiber to obtain a Gaussian beam profile. The output beam was collimated and reflected by a polychroic mirror (z488/633rpc) onto the back aperture of an oil immersion objective (NA=1.4, Olympus UPLSApo 100x). The sample holder with the glass slide and electrodes were mounted on a scanning stage (Physik Instrumente P-517.3CD) controlled by a nanopositioning system (Physik Instrumente E-710.3CD). The epifluorescence light was collected back through the same objective and focussed on a 50 μm pinhole for spatial filtering, then the light passed through an emission filter (z488/635m "dual"-band emission filter, Chroma). The fluorescence beam was re-collimated and focussed on single-photon avalanche photo diodes (SPCM AQRH-15, Perkin Elmer Inc., USA). The signal from the photo diode was recorded by a PicoHarp 300 (PicoQuant GmBH, Berlin, Germany) in time-tagged-time-resolved mode.

Data recording

A 20×20 μm^2 area of the sample surface functionalized with sparsely distributed ATTO655-labeled Azurin was scanned with 50 nm per pixel and with a dwell time of 1 ms per pixel. A typical fluorescence intensity image can be seen in Scheme-1. A constant potential of 200 mV (oxidizing) was applied by the electrochemical analyzer and an image of the same area taken after 2 min. Typically within one minute, the solution potential of the mixture of 0.1 mM ascorbate and 0.2 mM ferricyanide reaches the applied potential. Another image of the same area recorded at 0 mV (reducing). The two images were compared to identify the molecules that switch on-off at the two potentials (Scheme-1 (9 & 10)). The coordinates of the switching molecules were registered and an automatic recording was started. For each molecule, time traces were recorded for 30 s at different potentials between -100 mV and 100 mV. For observing dynamic of a single-molecule over longer period, time traces were recorded until the dye on it bleached or became dead. The Zn-azurin-ATTO655 was used

used as a control which doesn't show switching it's intensity at the above two potentials and time traces were recorded at the same potentials as Cu-azurin.

Data analysis

All the measurements resulted a huge amount data (more than 1000 time traces). Each time trace contains absolute arrival times of photons as well as arrival time with respect to excitation laser pulse. This enabled us to extract maximum information from the traces. To minimize human error and attain efficiency, codes were written (in python, matlab) to analyze all the traces exactly the same way. The code and data ca be found in the given link (will be provided during submission). Mainly three analysis were made on each trace. (i) Change points in the time traces were obtained using the changepoint algorithm[5] kindly provided by Prof. Haw Yang (Princeton University, USA). This method is binning free and doesn't require any prior knowledge of the underline kinetics. It determines the location of intensity changes based on the photon arrival times and the algorithm is recursively applied through the whole trace to find all the changes. Bayesian information criterion is used to find the number of states. Two states were predicted from long time traces and many molecules (2500 changepoints each) with more than 90% accuracy which was expected from FRET quenching mechanism and total signal that we have. For the rest of the traces, we set the number of states to be two in order to minimize the computation time. An example of change points and it's overlap with the real time trace can be seen in Figure-1. (ii) Autocorrelation of the time traces were performed by using SymPhoTime(PicoQuant) software. (iii) Further analysis of changepoint outputs and autocorrelation outputs were performed in Python. The details of the code including all the fitting functions can be found in the online repositories (will be provided during submission).

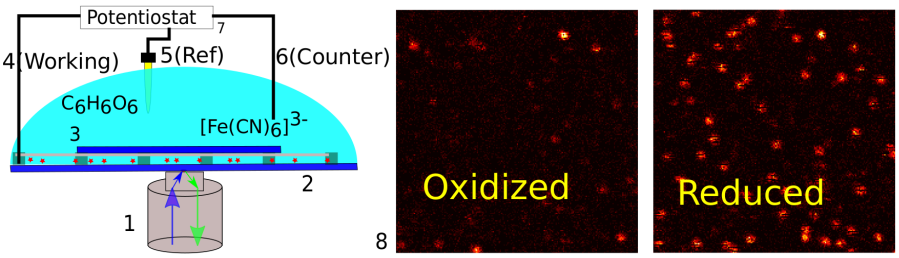

Scheme 1: The schematic picture of the confocal and electrochemical setup. **(1)** Objective through which light is irradiated on and collected from the sample. **(2)** The functionalized sample slide with on top the platinum grid and another small glass slide to press the grid on the sample slide, resulting in small confined volumes in the order of nanoliters. **(3)** The electron mediator solution consisting of 200 µM ferricyanide, 100 µM ascorbate in PBS (PH 7.4) buffer with a total volume of 4 mL. **(4)** The working electrode (Platinum wire) that is in contact with the platinum grid. **(5)** The saturated calomel reference electrode. **(6)** The Platinum wire (not touching the grid) as counter electrode. **(7)** The potentiostat (Model 800B Series Electrochemical Detector, CH Instruments) to which the electrodes are connected. **(8)** Top view of the sample slide and two images are showing the labeled Cu-Azurin reduced(brighter) and oxidized(dimmer).

Results and discussion

Time traces at different potentials

Active Cu-azurin molecules were identified from their fluorescence intensity images at the oxidizing (200 mV) and reducing conditions(0 mV). In reducing conditions, the image contains more brighter spots corresponding to Cu(I)-azurin-ATTO655 and more than 90 % of the molecules turned off in oxidizing conditions (Scheme-1(9)). The azurins on each sample slide showed active switching during the course of our experiment (up to two days) without any noticeable degradation. A set of active azurins were marked for recording and time traces at different potentials (between 100 mV and −100 mV) were measured on the `same molecules` for 30 s. Many of the labeled-protein bleached within recording at few potentials, but more than 50 % of the labeled-azurin survived at least five measurements (150 s) at different potentials. Longer measurements were possible due to the scavenging of oxygen in the solution. Before the time trace recording, the solution was exposed to negative potential for at least 1 hours. Ascorbate is known to scavenge oxygen[6] and get oxidized.

The oxidized ascorbate is reduced by the electrode and was again available to scavenge other oxygen molecules. In addition to the absence of oxygen, the ROXS mechanism was also in play. The reduction and oxidation of Cu-azurin made the dye switch on and off, hence the fluorescent dye spent less time on the bright state where it is more prone to bleach. This made possible the measurement of some traces more than 1000 s long.

Figure-1 shows time traces of a single Cu-azurin-ATTO655 at three different potentials.

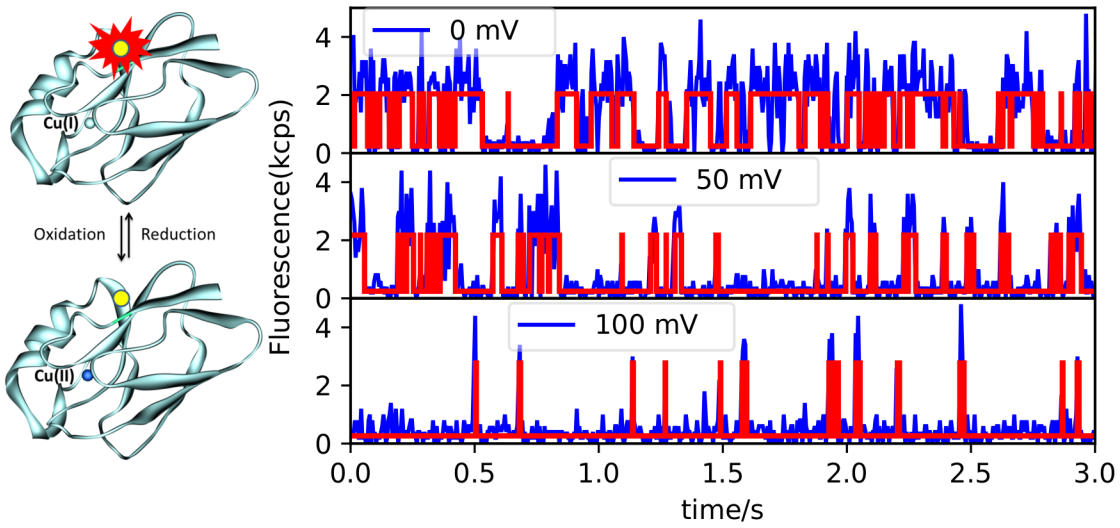

Figure 1: Time traces of Cu-Azurin labeled with ATTO655 at different potentials. The structure of the protein with properly positioned dye can be seen in the schematic picture in the left. In Cu(II) state (shown in bluish atom in the protein structure), the dye is non fluorescent because of FRET and in Cu(I) state (shown in gray atom), the dye is fluorescent. Notice the amount of time the protein spends on bright and dark state at different potentials. At lower potentials (e.g 0 mV) the protein is brighter most of the time because of the higher concentration of reductant.

Clearly the intensity changes from bright to dark and vise versa over the time which is also schematically shown in the left of Figure-1 with the protein structure. The dark state is due to the FRET from the dye to the Cu(II) absorption center.[7] Bulk measurements of the fluorescence intensity at completely oxidizing and completely reducing condition shows 90 % switching ratio (Figure-S2) for the lysine-122[2] labeled Cu-azurin-ATTO655. Also single-molecule measurement (Figure-S4) at a higher laser power (0.7 µW) shows more than 90 % switching which is consistent with the bulk measurements. The intensity of Cu(II)-state is

lower than Cu(I)-state, but higher than the background (bleached state). Also the Cu(II)-state has a shorter lifetime(0.3 ns than Cu(I)-state (1.9 ns), but longer than the instrument response function (0.1 ns). Both intensity and life time information reassure us that the dim-state we looking at is FRET quenched. Other blinking mechanism appears at lower potentials which will be discussed later. The high FRET efficiency is due to the small distance of the dye to the absorption center. This clear distinction between the on and off state was very important for our low laser power and lower signal measurement. At higher potential (100 mV), the protein spends most of the time in dark state and as the potential is lowered, the molecule spends more and more time on the bright state. As we lower the potential, the concentration of the reductant increases keeping the protein in Cu(I)-state for longer time. A control study with Zn-azurin-ATTO655 (Figure-S3 and Figure-S5) shows that the dye itself blinks below 40 mV due to photo-excited electron transfer. Zinc does not absorb light in the red and does not switch it's oxidation state. To leave out the complication in the analysis procedure, only potentials above 40 mV were considered for Cu-azurin-ATTO655 study.

Midpoint potential of single-azurins

Figure-2a shows the ratio between average off-time and average on-time plotted against the applied potential. The linear relationship of the log of the ratio with the potential can be modeled with the Nernst equation:

$$E = E_0 + \frac{k_B T}{ne} \ln\left(\frac{\bar{t}_{on}}{\bar{t}_{off}}\right) \tag{1}$$

where E is the applied potential, E_0 the mid-point potential, k_B the Boltzmann constant, T the absolute ambient temperature, n the number of electrons involved in the reaction, e the electron charge and $\bar{t}_{on}$, $\bar{t}_{off}$ the mean on and off times. The number of electrons involved

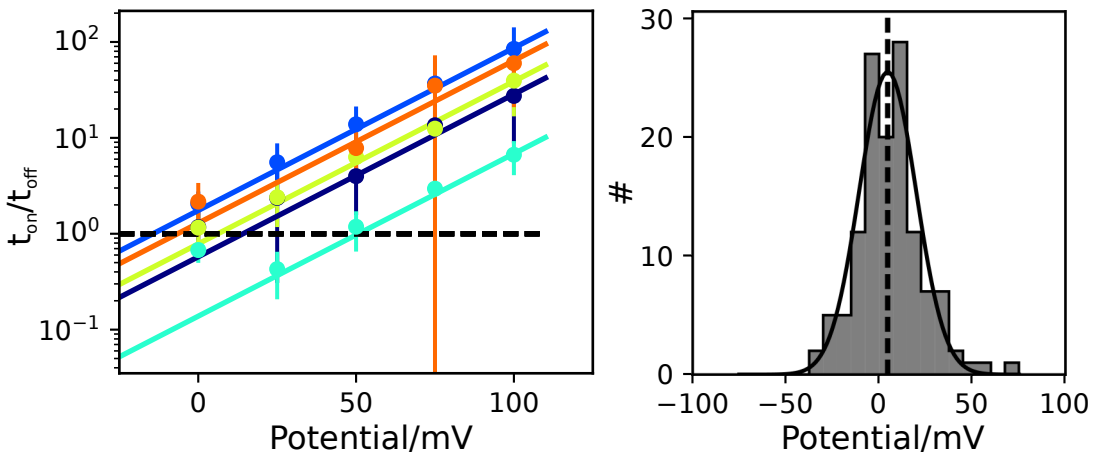

Figure 2: Ratio between on and off time as a function of applied potential for the same single-molecule. Different color represents different single-molecules. And the line connecting the data points is the Nernst fit for all the data points above 25 mV. The plot in the right is the histogram of midpoint potentials for 132 molecules with a Gaussian fit with a center value of 4.5 mV with respect to calomel electrode.

in the electron transfer was set to 1. The value of n was also found to be one from the ratio plot when the slope in the Nernst equation kept as free parameter (see Figure-S6). Each color represents a single-azurin and the solid line connecting the points is the Nernst-fit. Labeled proteins surviving at least three potentials above 40 mV were used for the fit. The potential at which the off-on ratio is 1 called midpoint potential which means the probability of finding the protein in Cu(I) and Cu(II) state are the same. The distribution of mid-point potentials(Figure-2b) from 132 molecules can be fitted by a Gaussian with a center value of $\left\langle E_0^{SM} \right\rangle = 4.5 \pm 1.2$ mV and a full width half maximum (fwhm) of $\sigma^{SM} = 36 \pm 3$ mV. The midpoint potential values are similar to previously reported values of 6 ± 0.6 mV with fwhm=150 mV where each E_0 was calculated from about 1000 molecules.[8] Another work reported $E_0 = 16\ mV$ with low surface coverage (100s of azurins) with a fwhm of 70 mV.[9] Recently for truly single-azurin, $E_0 = 12 \pm 3$ was reported with fwhm of 92 mV.[10]

A small width of distribution (36 mV) for single-azurin potentials in this work is obtained probably because of the way the proteins are functionalized to the surface. The azurin is attached to a peg-chain of length ∼20 nm. The peg-chain is attached to the surface through neutravidin. Such functionalization minimizes the interaction of the protein to the

surface. In all the previous experiment, the azurin was either non-specifically attached to the surface or attached through a very small linker (<1 nm). The surface interaction to different hydrophobic and electrostatic patches on the protein can alter the ET functionality of the enzyme.

Intermediate detection from on-off histogram

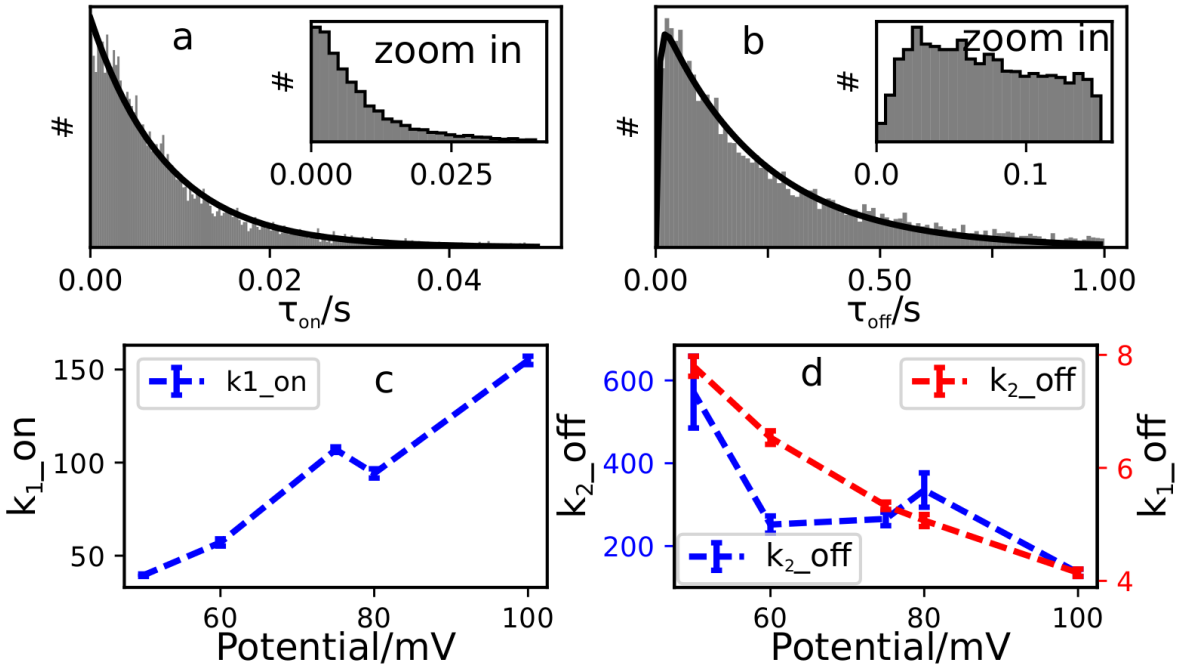

Figure 3: **Electron transfer rates** The histogram of on-times (a) and of off-times (b) of all the single-Cu-Azurin-ATTO655 at 100 mV with their zoomed in part in the inset. Notice the single exponential decay of on-times and the bi-exponential (with rise time) for the off-times. This indicates that reduction of Cu-Azurin occurs through an intermediate step while for oxidation the intermidiate state is not observable. The solid line is the corresponding fit to the distribution. (c) The rate constant for oxidation as a function of potential. (d) The rate constant for reduction as a function of redox potential, blue points correspond to the faster rate constant and the red represents the slow rate constant.

The on and off times of all the molecules at a certain potential were put together to see the over all distribution. Figure-3(a) shows the histogram of on times at 100 mV and the solid line is a fit with a single exponential with a time constant (k_{on}) of 155 s^{-1}. The on-time

represents the time the protein takes to get oxidized whose mechanism can be shown as:

$$\underset{\text{bright}}{\text{Cu(I)Azurin}} + \text{oxd} \underset{k_{-1}}{\overset{k_1}{\rightleftharpoons}} \underset{\text{dark}}{\text{Cu(II)Azurin}} + \text{red} \tag{2}$$

In contrast, the distribution of off-times shows non-exponential distribution with a rise time Figure-3(a). In the inset, the zoomed in part clearly shows that the probability of finding the protein with very short off-time is smaller. This distribution can be explained by Michaelis-Menten mechanism:

$$\underset{\text{dark}}{\text{Cu(II)Azurin}} + \text{red} \underset{k_{-1}}{\overset{k_1}{\rightleftharpoons}} \underset{\text{dark}}{\text{Cu(II)Azurin*red}} \xrightarrow{\text{k}_2} \underset{\text{bright}}{\text{Cu(I)Azurin}} + \text{oxd} \tag{3}$$

where k_1 is the pseudo-first order rate constant which depends on the concentration of reductant and k_2 is the zero order rate constant which should be independent of the concentration of the substrate. By assuming $k_{-1} = 0$, the probability of off time can be given as:[11]

$$P_{off}(t) = \frac{k_1 k_2}{k_2 - k_1}[exp(-k_1 t) - exp(-k_2 t)] \tag{4}$$

At 100 mV, k_1 for the reduction is 4.1 s^{-1} while k_2 is 135 s^{-1}. The rates were determined at different applied potential. A linear relationship is observed between the rate of oxidation and the solution potential (Figure-3(c)). This is in agreement with the first-order kinetic dependent on the concentration of substrate as the concentration of electron mediators vary exponentially with the solution potential. From the slope of the line, a rate constant of $9.4 \times 10^6\ M^{-1}s^{-1}$ for the oxidation is obtained. Similar linear relationship was observed for the k_1 of the reduction process as expected with a rate constant of $1.7 \times 10^5 M^{-1}s^{-1}$.

The rate constant (k_2) for the second step in the reduction process has a weak dependence on the solution reduction potential(Figure-3(d, blue)). The value is around $\sim 250 s^{-1}$ which is more than an order of magnitude smaller than the rate of intermediate formation.

Dynamics in ET rate

After looking at many single-azurins, we investigated a single-azurin for long time. Figure-4 shows the statistics of a single-azurin at 100 mV that survives for $\sim$1250 s. The distribution of on and off times are similar to that of many single-azurin distributions.

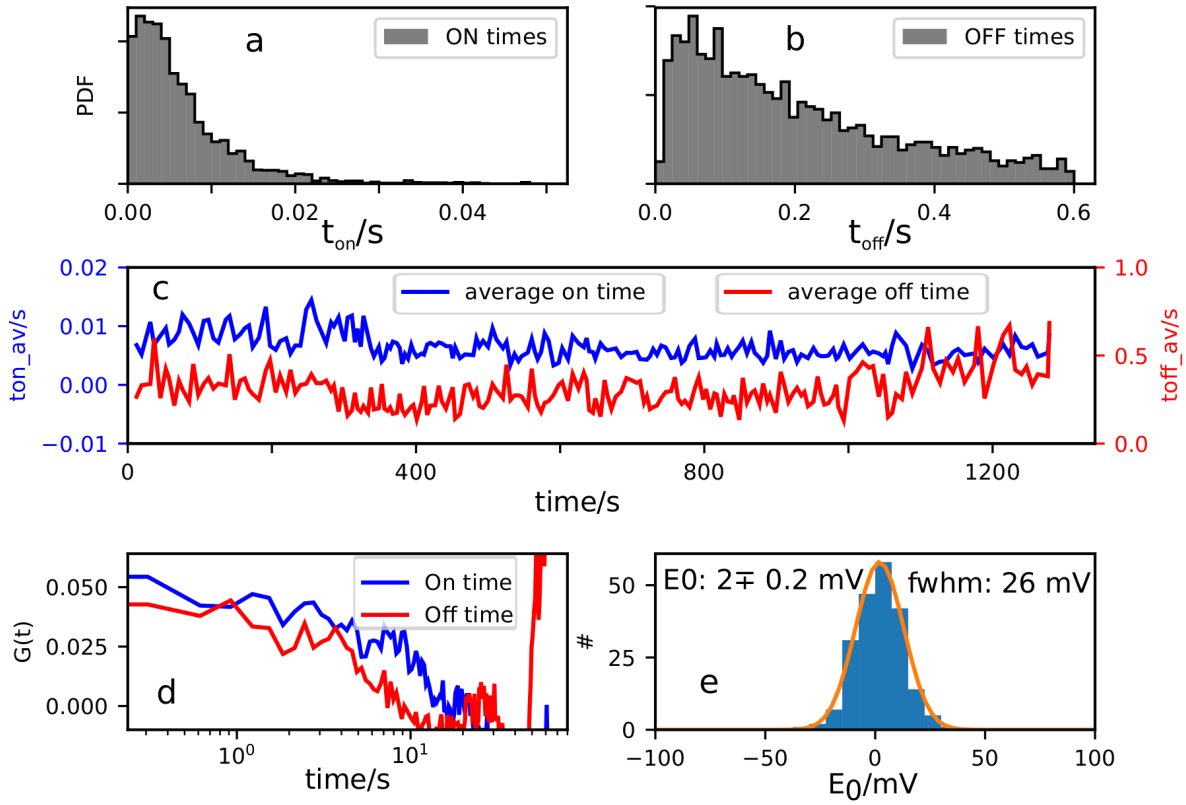

Figure 4: The histogram of on-times(a) and of off-times(b) of Cu-Azurin-ATTO655 showing rise time similar to many single-azurin distributions. (b) the trace of average on-times (blue) and average off-times (red). The average was calculated every 20 corresponding on or off times. The respective y-scales have the same color as the data points. (d) Autocorrelation of the traces in (c) and the color is matched to the color in the trace. (d) distribution of E_0 calculated from each average on and off time from the traces in (c)

The time trace was divided into small parts and average was calculated over every 20 on or off times. Figure-4 (c) shows the average on-times (blue) and average off-times (red) as a function of time. To our surprise, the fluctuations are not simply statistical noise rather seems correlated. The autocorrelations of the average traces show clear decay (Figure-4(d)) with decay times around 10s of seconds. This means that the rate at which the azurin

change between Cu(II) and Cu(I) state varies over time. Sometimes the frequency of the state-change is low and sometimes it is high. Such behaviors has been observed previously for other enzymes (β-galactosidase, flavoenzymes).[11–13] which can be termed as breathing in enzymes. A short on-time is followed be a short on-time and a longer on-time is followed by a longer on-time with the memory lasting over a characteristic time scale of $10s$ of seconds. According to the previous report, the breathing is a result of slow fluctuations in the structure over time. Azurin is a very small protein (14kDa) and the observation of such variation in ET shows that the ET is very sensitive to the changes in the structure.

Also mid-point potentials were calculated from each average on and average off times using Nernst equation(1). As both on and off times changes over time, mid-point potential too changes over time. The distribution of E_0 shows a center value of 2 ± 0.2 mV with a fwhm of 26 mV. This distribution of midpoint potential of a single-azurin over a long time is similar to the value of 36 mV obtained for many single-azurins.

Conclusion

The results presented here shows how to controllably switch the solution potential and determine the switching ratio of redox active azurin. By introducing non-interacting surface and long linker, very narrow distribution in the midpoint potential obtained. The distribution over many single-azurin was found to be very close to the distribution of a single-azurin over long time. The rate of intermediate formation for the reduction process has been observed conferring to Michaelis-Menten mechanism. The intermediate formation for the oxidation was too fast to be detected with our signal to noise ratio. In principle similar measurement at higher laser power and for many molecule should enable the detection of the intermediate if their is any. For the first time, correlated dynamics observed in the ET of very small azurin whose molecular mechanism still need to be deciphered.

References

(1) Kamp, M. v. d.; Hali, F.; Rosato, N.; Agro, A.; Canters, G. *Biochimica et biophysica acta* **1990**, *1019*, 283–92.

(2) Nicolardi, S.; Andreoni, A.; Tabares, L. C.; Burgt, Y. E. v. d.; Canters, G. W.; Deelder, A. M.; Hensbergen, P. J. *Analytical chemistry* **2012**, *84*, 2512–20.

(3) Gupta, A.; Nederlof, I.; Sottini, S.; Tepper, A. W. J. W.; Groenen, E. J. J.; Thomassen, E. A. J.; Canters, G. W. *Journal of the American Chemical Society* **2012**, *134*, 18213–18216.

(4) Zhang, W.; Caldarola, M.; Pradhan, B.; Orrit, M. *Angewandte Chemie International Edition* **2017**, *56*.

(5) Watkins, L. P.; Yang, H. *The Journal of Physical Chemistry B* **2005**, *109*, 617–628.

(6) Dave, R. I.; Shah, N. P. *International Dairy Journal* **1997**, *7*, 435–443.

(7) Kuznetsova, S.; Zauner, G.; Schmauder, R.; Mayboroda, O. A.; Deelder, A. M.; Aartsma, T. J.; Canters, G. W. *Analytical biochemistry* **2006**, *350*, 52–60.

(8) Davis, J.; Burgess, H.; Zauner, G.; Kuznetsova, S.; Salverda, J.; Aartsma, T.; Canters, G. *The journal of physical chemistry. B* **2006**, *110*, 20649–54.

(9) Salverda, J. M.; Patil, A. V.; Mizzon, G.; Kuznetsova, S.; Zauner, G.; Akkilic, N.; Canters, G. W.; Davis, J. J.; Heering, H. A.; Aartsma, T. J. *Angewandte Chemie (International ed. in English)* **2010**, *49*, 5776–9.

(10) Akkilic, N.; Grient, F. v. d.; Kamran, M.; Sanghamitra, N. J. M. *Chemical Communications* **2014**, *50*, 14523–14526.

(11) Lu, H. P.; Xun, L.; Xie, X. S. *Science* **1998**, *282*, 1877–1882.

(12) Kou, S. C.; Cherayil, B. J.; Min, W.; English, B. P.; Xie, X. S. *The Journal of Physical Chemistry B* **2005**, *109*, 19068–19081.

(13) English, B. P.; Min, W.; Oijen, A. M. v.; Lee, K. T.; Luo, G.; Sun, H.; Cherayil, B. J.; Kou, S. C.; Xie, X. S. *Nature chemical biology* **2006**, *2*, 87–94.